Topological Derivative for Linear Elastic Plate Bending Problems

A.A. Novotny[a], R.A. Feijóo[a], C. Padra[b] & E. Taroco[a]
[a]Laboratório Nacional de Computação Científica LNCC/MCT,
Av. Getúlio Vargas 333, 25651-075 Petrópolis - RJ, Brasil
[b]Centro Atómico Bariloche, 8400 Bariloche, Argentina

May 27, 2004

Abstract

This study concerns the application of the Topological-Shape Sensitivity Method as a systematic procedure to determine the Topological Derivative for linear elastic plate bending problems within the framework of Kirchhoff's kinematic approach. This method, based on classical Shape Sensitivity Analysis, leads to a constructive procedure to obtain the Topological Derivative. Utilizing the well known terminology of structural optimization, we adopt the total potential strain energy as the cost function and the equilibrium equation as the constraint. Variational formulation as well as the direct differentiation method are used to perform the shape derivative of the cost function. Finally, in order to obtain a uniform distribution of bending moments in several plate problems, the Topological Derivative was approximated, by the Finite Element Method, and used to find the best place to insert holes. A simple hard-kill like topology algorithm, which furnishes satisfactory qualitative results in agreement with those reported in the literature, is also shown.

1 Introduction

The Topological Derivative gives the sensitivity of a cost function when a small hole is introduced in the domain. More specifically, the idea is to make a perturbation on the domain Ω by subtracting a ball of radius ϵ, denoted by B_ϵ, centered in a point $\hat{\mathbf{x}} \in \Omega$. This originates a new domain $\Omega_\epsilon = \Omega - \overline{B}_\epsilon$. Therefore, if a cost function ψ defined in Ω is considered, then the Topological Derivative, here denoted by D_T, can be defined as

$$\psi(\Omega_\epsilon) = \psi(\Omega) + f(\epsilon) D_T + \mathcal{R}(f(\epsilon)). \tag{1}$$

In the expression above, $f(\epsilon)$ can be adopted as negative function which depends on the problem under analysis and such that $f(\epsilon) \to 0$ when $\epsilon \to 0$. $\mathcal{R}(f(\epsilon))$ contains all higher order terms than $f(\epsilon)$, that is, it satisfies

$$\lim_{\epsilon \to 0} \frac{\mathcal{R}(f(\epsilon))}{f(\epsilon)} = 0.$$

In general, ψ depends explicitly and implicitly on ϵ. The implicit dependence arises from the solution of the boundary value problem defined in Ω_ϵ. If this problem is elliptic, conditions in the whole boundary of Ω_ϵ must be imposed. Therefore, when B_ϵ is introduced, boundary conditions must also be defined on ∂B_ϵ.

The sensitivity of the total energy when a small hole is introduced in the domain can be seen, for example, in Germain & Muller [11]. Using this result, Schumacher [31] developed the bubble method for topological optimization. Then, Sokolowski & Żochowski [33, 34] and Garreau et al. [12, 13] extended this idea and the Topological Derivative concept was introduced.

Recently, the Topological Derivative has been recognized as a powerful tool to solve topology optimization problems (see [5], where 425 references concerning topology optimization of continuum structures are included). See also [4, 6, 20] and references therein. More recently, the potential

applications of the topological derivative to numerical methods for shape and topological optimum design were presented by Sokolowski & Żochowski [35]. Moreover, this publication also shows that the tools introduced in topological sensitivity analysis are closely related to the basic research in asymptotic analysis of solutions to boundary value problem under singular perturbations.

Extension of the topological derivative in order to include arbitrary shaped holes or inclusion with a perturbation of the physical properties of the material constituting the domain and its applications to Elasticity, Laplace, Poisson, Helmoltz, Stokes, Navier-Stokes equations are developed by Sokolowsky and his co-workers (see [32] and references therein) and by Masmoudi and his co-workers (see [15] and references therein). See also [1, 8, 14, 27, 28, 30, 35] for applications of the topological derivative to the above equations, inverse problems and material properties characterization.

To obtain D_T, an asymptotic analysis of the problem must be carrying out (see the publications refered at the end of this work). Following this approach and using the Dirichlet-to-Neumann map, Garreau et al.[12] introduce the Domain Truncation Method that can be used for singular problems such as those with Dirichlet boundary conditions imposed on ∂B_ϵ.

As mentioned by Masmoudi and his co-workers [15], asymptotic expansions are obtained using mathematical tools which are, in some sense, complicated. Then, their goal on that paper was to provide to engineers an easy way to obtain the derivation of topological asymptotic expansion using differential calculus under weak assumptions.

Following similar motivation, in [24] was proposed an other method to compute the Topological Derivative via Shape Sensitivity Analysis. This method, called Topological-Shape Sensitivity Method, allows to consider any kind of cost functions and any type of boundary conditions on the hole. This approach was applied for heat conduction problems [25], for the Poisson's problem considering a general set of boundary conditions on the holes [9], plane stress elasticity problems [10] and to compute the so-called Configurational Derivative [26].

Our aim in the present paper is to apply the Topological-Shape Sensitivity Method for performing the calculation of the topological derivative for Kirchhoff's plate bending problem. For the sake of completeness, in Section 2 we recall the Topological-Shape Sensitivity Method. In Section 3 we compute the Topological Derivative for Kirchhoff's plate bending problem, considering the total potential energy as the cost function and the state equation as the constraint. Finally and in order to obtain a new design in which the bending moments should be more uniformly distributed, in Section 4 the topological derivative is used to find the *best* place to insert holes for several plates with different boundary conditions and loads.

2 Topological-Shape Sensitivity Method

Let us consider an open bounded domain $\Omega \subset \mathbb{R}^2$ with a smooth boundary Γ. If the domain Ω is perturbed by introducing a small hole at an arbitrary point $\hat{\mathbf{x}} \in \Omega$, we have a new domain $\Omega_\epsilon = \Omega - \overline{B}_\epsilon$, whose boundary is denoted by $\Gamma_\epsilon = \Gamma \cup \partial B_\epsilon$, where $\overline{B}_\epsilon = B_\epsilon \cup \partial B_\epsilon$ is a ball of radius ϵ centered at the point $\hat{\mathbf{x}} \in \Omega$. Thus, we have the original domain without hole Ω and the new one Ω_ϵ with a small hole B_ϵ. Considering Eq. (1), the Topological Derivative can be re-written as [13]

$$D_T(\hat{\mathbf{x}}) = \lim_{\epsilon \to 0} \frac{\psi(\Omega_\epsilon) - \psi(\Omega)}{f(\epsilon)} . \tag{2}$$

In [25] the authors proposed a method, called Topological-Shape Sensitivity Method, which allows us to use the whole mathematical framework (and results) developed for Shape Sensitivity Analysis (see [3, 16, 17, 22, 29, 36, 37, 39] and references therein) to compute the Topological Derivative. The main result obtained in [25] is given by the following theorem:

Theorem 1 *Let $f(\epsilon)$ be a function chosen in order to $0 < |D_T(\hat{\mathbf{x}})| < \infty$, then the Topological Derivative given by Eq. (2) can be written as*

$$D_T(\hat{\mathbf{x}}) = \lim_{\epsilon \to 0} \frac{1}{f'(\epsilon)\,|v_n|} \frac{d}{d\tau} \psi(\Omega_\tau) \Big|_{\tau=0} , \tag{3}$$

where $\tau \in \mathbb{R}$ is used to parameterize the domain. That is, for τ small enough, we have

$$\Omega_\tau := \left\{ \mathbf{x}_\tau \in \mathbb{R}^2 : \exists\ \mathbf{x} \in \Omega_\epsilon, \quad \mathbf{x}_\tau = \mathbf{x} + \tau \mathbf{v}, \quad \mathbf{x}_\tau|_{\tau=0} = \mathbf{x} \quad \textit{and} \quad \Omega_\tau|_{\tau=0} = \Omega_\epsilon \right\} ,$$

being $\mathbf{v}$ *the* shape change velocity *defined by*

$$\begin{cases} \mathbf{v} = v_n \mathbf{n} & \textit{with } v_n < 0 \textit{ constant on } \partial B_\epsilon, \\ \mathbf{v} = \mathbf{0} & \textit{on } \Gamma, \end{cases} \tag{4}$$

where v_n is the normal component of the velocity. In addition,

$$\frac{d}{d\tau} \psi(\Omega_\tau) \Big|_{\tau=0} = \lim_{\tau \to 0} \frac{\psi(\Omega_\tau) - \psi(\Omega_\epsilon)}{\tau} . \tag{5}$$

is the shape sensitivity of the cost function in relation to the domain perturbation characterized by $\mathbf{v}$.

Proof. The reader interested in the proof of this result may refer to [9, 25] ■

This theorem points out that the Topological Derivative may be obtained through the Shape Sensitivity Analysis of the cost function (Topological-Shape Sensitivity Method). Therefore, results from Shape Sensitivity Analysis can be used to calculate the Topological Derivative in a constructive way considering Eq. (3).

3 Topological Derivative in thin plate bending problem

In the present section, we compute the Topological Derivative for thin elastic plate bending problem within the framework of Kirchhoff's simplified assumptions. Using the well known terminology of structural optimization, we adopt the total potential energy as the cost function and the equilibrium equation as the constraint.

3.1 Mechanical model

Let us review briefly in this section the theory of elastic plates under Kirchhoff's assumptions. This approach, known in solid mechanics as first order plate theory, reduces the analysis to a two-dimensional problem over the middle surface of the plate. Thus, consider a flat plate, with thickness $\rho \in \mathbb{R}^+$ (admitted constant for the sake of simplicity), characterized by the two-dimensional domain $\Omega_\epsilon \subset \mathbb{R}^2$ ($\Omega_\epsilon = \Omega - \overline{B}_\epsilon$), which may be adopted as the reference domain, submitted to bending effects. In order to model this phenomenon Kirchhoff developed, in 1850, a theory based on the following *ad-hoc* kinematic assumptions:

> *The normal fibers to the middle plane of the plate remain normal during deformation and do not suffer variations in their length.*

Consequently, both transversal shear and normal deformations are null. This fact limits the application of Kirchhoff's approach on plates whose deflections are small in relation to the thickness ρ. Note that in the presence of concentrated loads or defects like cracks, additional care will be necessary since transversal shear deformation may be significative.

Utilizing kinematic assumptions introduced by Kirchhoff and adopting the constitutive relation for a linear elastic isotropic material, we respectively have the following strain-displacement and stress-strain relations

$$\mathbf{E}_\epsilon = -\nabla\nabla u_\epsilon \qquad \text{and} \qquad \mathbf{M}_\epsilon = \mathbf{C}\mathbf{E}_\epsilon = -\mathbf{C}\nabla\nabla u_\epsilon \ , \tag{6}$$

where the scalar field u_ϵ denotes the transverse displacement (deflexion), the symmetric tensor $\mathbf{E}_\epsilon$ is the generalized flexural strain which represents the change of curvature of the plate, the symmetric tensor $\mathbf{M}_\epsilon$ is the generalized stress tensor that represents the bending moment in the middle plane of the plate and $\mathbf{C} = \mathbf{C}^T$ is the forth order elasticity tensor, which is given by

$$\mathbf{C} = \frac{E\rho^3}{12\,(1-\nu^2)}\left[(1-\nu)\,\mathbf{II} + \nu\,(\mathbf{I}\otimes\mathbf{I})\right] \ , \tag{7}$$

being $\mathbf{I}$ and $\mathbf{II}$ respectively the second and forth order identity tensors, E the Young's modulus, ν the Poisson's ratio and ρ the thickness.

Therefore, in terms of the primal variable u_ϵ, the equilibrium of the plate can be described by the following variational problem: find $u_\epsilon \in \mathcal{U}_\epsilon$, such that

$$a_\epsilon\,(u_\epsilon,\eta_\epsilon) = l_\epsilon\,(\eta_\epsilon) \qquad \forall \eta_\epsilon \in \mathcal{V}_\epsilon \ , \tag{8}$$

where

$$a_\epsilon\,(u_\epsilon,\eta_\epsilon) = \int_{\Omega_\epsilon} \mathbf{C}\nabla\nabla u_\epsilon \cdot \nabla\nabla\eta_\epsilon \, d\Omega_\epsilon \tag{9}$$

$$l_\epsilon\,(\eta_\epsilon) = \int_{\Omega_\epsilon} b\eta_\epsilon \, d\Omega_\epsilon + \int_{\Gamma_N}\left(\bar{q}\eta_\epsilon + \bar{m}\frac{\partial\eta_\epsilon}{\partial n}\right) d\Gamma + \sum_{i=1}^{nv} \bar{Q}_{v_i}\eta_\epsilon(\mathbf{x}_{v_i}) \quad \forall \eta_\epsilon \in \mathcal{V}_\epsilon \ , \tag{10}$$

being $\mathcal{U}_\epsilon$ the set of admissible displacements and $\mathcal{V}_\epsilon$ the space of admissible displacements variations, which are respectively defined by

$$\mathcal{U}_\epsilon := \left\{ u_\epsilon \in H^2\,(\Omega_\epsilon) : u_\epsilon|_{\Gamma_D} = \bar{u} \text{ and } \tfrac{\partial u_\epsilon}{\partial n}\big|_{\Gamma_D} = \bar{\theta} \right\} \ ,$$

$$\mathcal{V}_\epsilon := \left\{ \eta_\epsilon \in H^2\,(\Omega_\epsilon) : \eta_\epsilon|_{\Gamma_D} = 0 \text{ and } \tfrac{\partial \eta_\epsilon}{\partial n}\Big|_{\Gamma_D} = 0 \right\} \ ,$$

where Γ_D and Γ_N respectively are Dirichlet and Neumann boundaries such that $\Gamma = \Gamma_D \cup \Gamma_N$, with $\Gamma_D \cap \Gamma_N = \emptyset$; $\bar{u}$ is the displacement and $\bar{\theta}$ the rotation, both prescribed on Γ_D. Moreover, b, $\bar{q}$, $\bar{m}$ and $\bar{Q}_{v_i}$ are the system of forces compatible with Kirchhoff's approach, where b is the transverse force over the middle plane Ω_ϵ, $\bar{q}$ the transverse shear load and $\bar{m}$ is the moment, both prescribed on Γ_N; $\bar{Q}_{v_i}$ is the transverse shear load concentrated at the point $\mathbf{x}_{v_i} \in \Gamma_N$ in which there is some discontinuity (vertex, for instance) and nv represents the total number of points $\mathbf{x}_{v_i}$.

The Euler-Lagrange equation as well as the boundary conditions associated to the variational problem, (Eq. 8), are given by the following forth order boundary-value problem:

$$\left\{\begin{array}{lll}
\text{Find } u_\epsilon, \text{ such that} & & \\
-\text{div}\,(\text{div}\mathbf{M}_\epsilon) = b & \text{in} & \Omega_\epsilon \\
\left.\begin{array}{l} u_\epsilon = \bar{u} \\ \dfrac{\partial u_\epsilon}{\partial n} = \bar{\theta} \end{array}\right\} & \text{on} & \Gamma_D \\
\left.\begin{array}{l} \dfrac{\partial M_\epsilon^{tn}}{\partial t} + \text{div}\mathbf{M}_\epsilon\cdot\mathbf{n} = \bar{q} \\ -M_\epsilon^{nn} = \bar{m} \end{array}\right\} & \text{on} & \Gamma_N \\
-[\![M_\epsilon^{tn}]\!] = \bar{Q}_{v_i} & \text{on} & \mathbf{x}_{v_i} \in \Gamma_N, \quad i = 1, ..., nv \\
\left.\begin{array}{l} \dfrac{\partial M_\epsilon^{tn}}{\partial t} + \text{div}\mathbf{M}_\epsilon\cdot\mathbf{n} = 0 \\ -M_\epsilon^{nn} = 0 \end{array}\right\} & \text{on} & \partial B_\epsilon
\end{array}\right. \ . \tag{11}$$

It should be noted that we can decompose the stress tensor $\mathbf{M}_\epsilon$ along the boundary Γ_ϵ as follows

$$\mathbf{M}_\epsilon = M_\epsilon^{nn}\,(\mathbf{n}\otimes\mathbf{n}) + M_\epsilon^{nt}\,(\mathbf{n}\otimes\mathbf{t}) + M_\epsilon^{tn}\,(\mathbf{t}\otimes\mathbf{n}) + M_\epsilon^{tt}\,(\mathbf{t}\otimes\mathbf{t})\ , \tag{12}$$

where $\mathbf{n}$ and $\mathbf{t}$ are respectively the outward normal and tangential unit vectors ($\mathbf{n}\cdot\mathbf{t}=0$) defined on Γ_ϵ.

Moreover, according to Kirchhoff's approach, the total potential energy of the plate in the reference configuration, Ω_ϵ, may be written in the following compact form

$$\psi(\Omega_\epsilon) := \Psi_\epsilon\,(u_\epsilon) = \frac{1}{2}a_\epsilon\,(u_\epsilon, u_\epsilon) - l_\epsilon\,(u_\epsilon)\ , \tag{13}$$

where the first term represents the total strain energy stored in the plate and the second term represents the work of the external loads.

Since the equilibrium of the plate must be verified in all perturbed configuration Ω_τ, the corresponding transverse displacement u_τ satisfies the following variational problem: find $u_\tau \in \mathcal{U}_\tau$, such that

$$a_\tau\,(u_\tau,\eta_\tau) = l_\tau\,(\eta_\tau) \qquad \forall\eta_\tau \in \mathcal{V}_\tau \text{ and } \forall\tau \geq 0\ , \tag{14}$$

where $\mathcal{U}_\tau$ is the set of admissible displacements and $\mathcal{V}_\tau$ is the space of admissible displacement variations, both defined on the perturbed domain Ω_τ. In addition, $a_\tau\,(u_\tau,\eta_\tau)$ and $l_\tau\,(\eta_\tau)$ are given, respectively, by

$$a_\tau\,(u_\tau,\eta_\tau) = \int_{\Omega_\tau} \mathbf{C}\nabla_\tau\nabla_\tau u_\tau \cdot \nabla_\tau\nabla_\tau\eta_\tau\, d\Omega_\tau\ , \tag{15}$$

$$l_\tau\,(\eta_\tau) = \int_{\Omega_\tau} b\eta_\tau\, d\Omega_\tau + \int_{\Gamma_N}\left(\bar{q}\eta_\tau + \bar{m}\frac{\partial\eta_\tau}{\partial n}\right)d\Gamma + \sum_{i=1}^{nv}\bar{Q}_{v_i}\eta_\tau(\mathbf{x}_{v_i})\ , \tag{16}$$

where $\nabla_\tau := \frac{\partial}{\partial\mathbf{x}_\tau}(\cdot)$.

It should be noted that for the sake of simplicity, we have assumed that the parameters E, ρ, ν, $\bar{u}$, $\bar{\theta}$, b, $\bar{q}$, $\bar{m}$ and $\bar{Q}_{v_i}$ are constants in relation to the perturbation characterized by τ.

Similar to Eq. 13, the total potential energy of the plate in the perturbed configuration Ω_τ is given by

$$\psi(\Omega_\tau) := \Psi_\tau\,(u_\tau) = \frac{1}{2}a_\tau\,(u_\tau, u_\tau) - l_\tau\,(u_\tau)\ . \tag{17}$$

3.2 Shape Sensitivity Analysis

Now, we will focus our attention on the shape sensitivity analysis of a plate when the size of a small circular hole changes, specifically when the radius of the hole is perturbed. The calculation of the shape derivative will be performed considering the total potential energy as the cost function written in the perturbed configuration Ω_τ, that is Eq. (17), which we can express as

$$\begin{aligned}\Psi_\tau\,(u_\tau) := &-\frac{1}{2}\int_{\Omega_\tau}\mathbf{M}_\tau\cdot\nabla_\tau\nabla_\tau u_\tau\, d\Omega_\tau \\ &-\int_{\Omega_\tau} bu_\tau\, d\Omega_\tau - \int_{\Gamma_N}\left(\bar{q}u_\tau + \bar{m}\frac{\partial u_\tau}{\partial n}\right)d\Gamma - \sum_{i=1}^{nv}\bar{Q}_{v_i}u_\tau(\mathbf{x}_{v_i})\ .\end{aligned} \tag{18}$$

Once the cost function (Eq. 18) is characterized we may apply the direct differentiation method to obtain the shape derivative, in other words the derivative with respect to τ, that is

$$\frac{d}{d\tau}\Psi_\tau\,(u_\tau) = \frac{1}{2}\frac{d}{d\tau}a_\tau\,(u_\tau, u_\tau) - \frac{d}{d\tau}l_\tau\,(u_\tau)\ . \tag{19}$$

Since the elasticity tensor $\mathbf{C}$ is symmetric, from the Reynolds' transport theorem, the total derivative of the bilinear form $a_\tau\left(u_\tau,u_\tau\right)$, at $\tau=0$, becomes

$$\left.\frac{da_\tau}{d\tau}\right|_{\tau=0} = -\int_{\Omega_\epsilon}\left[2\mathbf{M}_\epsilon\cdot\left.\frac{d}{d\tau}\left(\nabla_\tau\nabla_\tau u_\tau\right)\right|_{\tau=0}+\mathbf{M}_\epsilon\cdot\nabla\nabla u_\epsilon\,\mathrm{div}\,\mathbf{v}\right]d\Omega_\epsilon\;, \tag{20}$$

where the total derivative of the second order gradient of a scalar field is given by

$$\begin{aligned}\left.\frac{d}{d\tau}\left(\nabla_\tau\nabla_\tau u_\tau\right)\right|_{\tau=0} &= \nabla\left.\frac{d}{d\tau}\left(\nabla_\tau u_\tau\right)\right|_{\tau=0}-\left(\nabla\nabla u_\epsilon\right)\nabla\mathbf{v}\\ &= -\nabla\left(\nabla\mathbf{v}^T\nabla u_\epsilon\right)-\left(\nabla\nabla u_\epsilon\right)\nabla\mathbf{v}+\nabla\nabla\dot{u}_\epsilon\;,\end{aligned} \tag{21}$$

being $\dot{(\cdot)}$ used to denote

$$\dot{(\cdot)} := \left.\frac{d}{d\tau}\left(\cdot\right)\right|_{\tau=0}\;.$$

Next, we use the following tensorial relations

$$\mathrm{div}\left(\mathbf{M}_\epsilon^T\nabla\mathbf{v}^T\nabla u_\epsilon\right)=\mathbf{M}_\epsilon\cdot\nabla\left(\nabla\mathbf{v}^T\nabla u_\epsilon\right)+\mathrm{div}\mathbf{M}_\epsilon\cdot\nabla\mathbf{v}^T\nabla u_\epsilon\;,$$

$$\mathrm{div}\mathbf{M}_\epsilon\cdot\nabla\mathbf{v}^T\nabla u_\epsilon=\nabla\mathbf{v}\,\mathrm{div}\mathbf{M}_\epsilon\cdot\nabla u_\epsilon=\left(\nabla u_\epsilon\otimes\mathrm{div}\mathbf{M}_\epsilon\right)\cdot\nabla\mathbf{v}\;,$$

to obtain

$$\mathbf{M}_\epsilon\cdot\nabla\left(\nabla\mathbf{v}^T\nabla u_\epsilon\right)=\mathrm{div}\left(\mathbf{M}_\epsilon\nabla\mathbf{v}^T\nabla u_\epsilon\right)-\left(\nabla u_\epsilon\otimes\mathrm{div}\mathbf{M}_\epsilon\right)\cdot\nabla\mathbf{v}\;, \tag{22}$$

and we also recall the definition of the transpose tensor, to write

$$\mathbf{M}_\epsilon\cdot\left(\nabla\nabla u_\epsilon\right)\nabla\mathbf{v}=\left(\nabla\nabla u_\epsilon\right)^T\mathbf{M}_\epsilon\cdot\nabla\mathbf{v}\;. \tag{23}$$

Then, combining Eqs. (21, 22 and 23), follows

$$\begin{aligned}\mathbf{M}_\epsilon\cdot\left.\frac{d}{d\tau}\left(\nabla_\tau\nabla_\tau u_\tau\right)\right|_{\tau=0} =& -\left(\nabla\nabla u_\epsilon\right)\mathbf{M}_\epsilon\cdot\nabla\mathbf{v}+\left(\nabla u_\epsilon\otimes\mathrm{div}\mathbf{M}_\epsilon\right)\cdot\nabla\mathbf{v}\\ &-\mathrm{div}\left(\mathbf{M}_\epsilon\nabla\mathbf{v}^T\nabla u_\epsilon\right)+2\mathbf{M}_\epsilon\cdot\nabla\nabla\dot{u}_\epsilon\;.\end{aligned} \tag{24}$$

If we insert the result given by Eq. (24) into Eq. (20) and apply the divergence theorem, remembering that $\mathbf{v}=\mathbf{0}$ on $\Gamma=\Gamma_D\cup\Gamma_N$, the derivative of the bilinear form becomes

$$\begin{aligned}\left.\frac{da_\tau}{d\tau}\right|_{\tau=0} =& -2\int_{\Omega_\epsilon}\left[\frac{1}{2}\left(\mathbf{M}_\epsilon\cdot\nabla\nabla u_\epsilon\right)\mathbf{I}-\left(\nabla\nabla u_\epsilon\right)\mathbf{M}_\epsilon+\nabla u_\epsilon\otimes\mathrm{div}\mathbf{M}_\epsilon\right]\cdot\nabla\mathbf{v}\,d\Omega_\epsilon\\ &+2\int_{\partial B_\epsilon}\left(\mathbf{M}_\epsilon\nabla\mathbf{v}^T\nabla u_\epsilon\right)\cdot\mathbf{n}\,d\partial B_\epsilon+2a_\epsilon\left(u_\epsilon,\dot{u}_\epsilon\right)\;.\end{aligned} \tag{25}$$

Likewise, the total derivative of the functional $l_\tau\left(u_\tau\right)$, at $\tau=0$, may be written as

$$\left.\frac{dl_\tau}{d\tau}\right|_{\tau=0}=\int_{\Omega_\epsilon}\left(bu_\epsilon\right)\mathbf{I}\cdot\nabla\mathbf{v}\,d\Omega_\epsilon+l_\epsilon\left(\dot{u}_\epsilon\right)\;. \tag{26}$$

Thus, substituting Eqs. (25, 26) in Eq. (19) and considering that u_ϵ satisfies Eq. (8), and since $\dot{u}_\epsilon\in\mathcal{V}_\epsilon$, the shape derivative of the cost function at $\tau=0$ becomes

$$\left.\frac{d\Psi_\tau}{d\tau}\right|_{\tau=0}=\int_{\Omega_\epsilon}\boldsymbol{\Sigma}_\epsilon\cdot\nabla\mathbf{v}\,d\Omega_\epsilon+\int_{\partial B_\epsilon}\mathbf{M}_\epsilon\mathbf{n}\cdot\nabla\mathbf{v}^T\nabla u_\epsilon\,d\partial B_\epsilon\;, \tag{27}$$

where the energy shape change tensor $\boldsymbol{\Sigma}_\epsilon$, given by

$$\boldsymbol{\Sigma}_\epsilon = -\frac{1}{2}\left(\mathbf{M}_\epsilon \cdot \nabla\nabla u_\epsilon + 2bu_\epsilon\right)\mathbf{I} + \left(\nabla\nabla u_\epsilon\right)\mathbf{M}_\epsilon - \nabla u_\epsilon \otimes \mathrm{div}\mathbf{M}_\epsilon \,, \tag{28}$$

can be seen as an extension of the Eshelby's energy-momentum tensor (see for instance [7, 37]) for elastic plates within the framework of Kirchhoff's approach. The energy momentum tensor was first introduced by Eshelby into elastostatics of three-dimensional bodies in the context of infinitesimal deformations. This tensor also plays a central role in the same author's development of continuum approach when studying defects in solid media.

Moreover, it is well known that shape derivative only depends on the value of $\mathbf{v}$ at the boundary. In order to assess the shape derivative as a boundary integral we recall the following tensorial relation

$$\mathrm{div}(\boldsymbol{\Sigma}_\epsilon^T \mathbf{v}) = \boldsymbol{\Sigma}_\epsilon \cdot \nabla\mathbf{v} + \mathrm{div}\boldsymbol{\Sigma}_\epsilon \cdot \mathbf{v} \,. \tag{29}$$

Next, combining Eq. (27) and Eq. (29) and making further use of the divergence theorem, yields

$$\left.\frac{d\Psi_\tau}{d\tau}\right|_{\tau=0} = \int_{\Gamma_\epsilon} \boldsymbol{\Sigma}_\epsilon\mathbf{n}\cdot\mathbf{v}\, d\Gamma_\epsilon + \int_{\partial B_\epsilon} \mathbf{M}_\epsilon\mathbf{n}\cdot\nabla\mathbf{v}^T\nabla u_\epsilon\, d\partial B_\epsilon - \int_{\Omega_\epsilon} \mathrm{div}\boldsymbol{\Sigma}_\epsilon\cdot\mathbf{v}\, d\Omega_\epsilon \,. \tag{30}$$

Since u_ϵ satisfies Eq. (8), $\dot{u}_\epsilon \in \mathcal{V}_\epsilon$ and remembering that $\mathbf{v}$ is an arbitrary velocity field, then it is straightforward to verify that

$$\int_{\Omega_\epsilon} \mathrm{div}\boldsymbol{\Sigma}_\epsilon\cdot\mathbf{v}\; d\Omega_\epsilon = 0 \quad \forall\ \mathbf{v} \quad \Leftrightarrow \quad \mathrm{div}\boldsymbol{\Sigma}_\epsilon = \mathbf{0} \,. \tag{31}$$

Thus, recalling the definition of the velocity field given by Eq. (4) and inserting Eq. (31) into Eq. (30), the shape derivative of the cost function reduces to an integral along the boundary ∂B_ϵ, that is

$$\left.\frac{d\Psi_\tau}{d\tau}\right|_{\tau=0} = v_n \int_{\partial B_\epsilon} \left(\boldsymbol{\Sigma}_\epsilon\mathbf{n}\cdot\mathbf{n} + \mathbf{M}_\epsilon\mathbf{n}\cdot\nabla\mathbf{n}^T\nabla u_\epsilon\right) d\partial B_\epsilon \,, \tag{32}$$

where

$$\boldsymbol{\Sigma}_\epsilon\mathbf{n}\cdot\mathbf{n} = -\frac{1}{2}\mathbf{M}_\epsilon\cdot\nabla\nabla u_\epsilon - bu_\epsilon + \mathbf{M}_\epsilon\mathbf{n}\cdot\left(\nabla\nabla u_\epsilon\right)^T\mathbf{n} - \left(\mathrm{div}\mathbf{M}_\epsilon\cdot\mathbf{n}\right)\left(\nabla u_\epsilon\cdot\mathbf{n}\right) \,.$$

If we consider the following tensorial relations

$$\begin{aligned} \nabla\left(\nabla u_\epsilon\cdot\mathbf{n}\right) &= \left(\nabla\nabla u_\epsilon\right)^T\mathbf{n} + \nabla\mathbf{n}^T\nabla u_\epsilon \,, \\ \mathbf{M}_\epsilon\mathbf{n}\cdot\left(\nabla\nabla u_\epsilon\right)^T\mathbf{n} &= \mathbf{M}_\epsilon\mathbf{n}\cdot\nabla\left(\nabla u_\epsilon\cdot\mathbf{n}\right) - \mathbf{M}_\epsilon\mathbf{n}\cdot\nabla\mathbf{n}^T\nabla u_\epsilon \,, \end{aligned}$$

we may write

$$\left.\frac{d\Psi_\tau}{d\tau}\right|_{\tau=0} = -v_n \int_{\partial B_\epsilon} \left[\frac{1}{2}\mathbf{M}_\epsilon\cdot\nabla\nabla u_\epsilon + bu_\epsilon + \left(\mathrm{div}\mathbf{M}_\epsilon\cdot\mathbf{n}\right)\left(\nabla u_\epsilon\cdot\mathbf{n}\right) - \mathbf{M}_\epsilon\mathbf{n}\cdot\nabla\left(\nabla u_\epsilon\cdot\mathbf{n}\right)\right] d\partial B_\epsilon \,. \tag{33}$$

In addition, when u_ϵ is defined on ∂B_ϵ, we can verify that

$$\nabla\left(\nabla u_\epsilon\cdot\mathbf{n}\right) = \frac{\partial}{\partial n}\left(\frac{\partial u_\epsilon}{\partial n}\right)\mathbf{n} + \frac{\partial}{\partial t}\left(\frac{\partial u_\epsilon}{\partial n}\right)\mathbf{t}$$

and, from Eq. (12), we obtain

$$\mathbf{M}_\epsilon\mathbf{n} = M_\epsilon^{nn}\mathbf{n} + M_\epsilon^{tn}\mathbf{t} \,,$$

thus

$$\mathbf{M}_\epsilon\mathbf{n}\cdot\nabla\left(\nabla u_\epsilon\cdot\mathbf{n}\right) = M_\epsilon^{nn}\frac{\partial^2 u_\epsilon}{\partial n^2} + M_\epsilon^{tn}\frac{\partial}{\partial t}\left(\frac{\partial u_\epsilon}{\partial n}\right) \,. \tag{34}$$

Substituting the result given by Eq. (34) in Eq. (33) and integrating by parts, we have

$$\begin{aligned}\left.\frac{d\Psi_\tau}{d\tau}\right|_{\tau=0} &= -v_n\int_{\partial B_\epsilon}\left[\frac{1}{2}\mathbf{M}_\epsilon\cdot\nabla\nabla u_\epsilon + bu_\epsilon - M_\epsilon^{nn}\frac{\partial^2 u_\epsilon}{\partial n^2}\right.\\ &\quad\left.+\left(\mathrm{div}\mathbf{M}_\epsilon\cdot\mathbf{n}\right)\frac{\partial u_\epsilon}{\partial n} - M_\epsilon^{tn}\frac{\partial}{\partial t}\left(\frac{\partial u_\epsilon}{\partial n}\right)\right]d\partial B_\epsilon\\ &= -v_n\int_{\partial B_\epsilon}\left[\frac{1}{2}\mathbf{M}_\epsilon\cdot\nabla\nabla u_\epsilon + bu_\epsilon - M_\epsilon^{nn}\frac{\partial^2 u_\epsilon}{\partial n^2}\right.\\ &\quad\left.+\left(\frac{\partial M_\epsilon^{tn}}{\partial t} + \mathrm{div}\mathbf{M}_\epsilon\cdot\mathbf{n}\right)\frac{\partial u_\epsilon}{\partial n}\right]d\partial B_\epsilon\,. \end{aligned} \tag{35}$$

Considering homogeneous Neumann boundary condition on ∂B_ϵ (see Eq. 11), the shape derivative of the cost function given by Eq. (35) becomes

$$\left.\frac{d\Psi_\tau}{d\tau}\right|_{\tau=0} = v_n\int_{\partial B_\epsilon}\left(\frac{1}{2}\mathbf{M}_\epsilon\cdot\mathbf{E}_\epsilon - bu_\epsilon\right)d\partial B_\epsilon\,. \tag{36}$$

3.3 Topological Derivative Calculation

From Theorem 1 and the previous shape sensitivity result given by Eq. (36), the Topological Derivative becomes

$$D_T\left(\hat{\mathbf{x}}\right) = -\lim_{\epsilon\to 0}\frac{1}{f'\left(\epsilon\right)}\int_{\partial B_\epsilon}\left(\frac{1}{2}\mathbf{M}_\epsilon\cdot\mathbf{E}_\epsilon - bu_\epsilon\right)d\partial B_\epsilon\,, \tag{37}$$

where $\mathrm{sign}\left(v_n\right) = -1$, was adopted for an expansion on the hole.

Next, to express the Topological Derivative as a function of the stress, we recall the inverse of the constitutive relation ($\mathbf{E}_\epsilon = \mathbf{C}^{-1}\mathbf{M}_\epsilon$), the symmetry of the bending moment tensor $\mathbf{M}_\epsilon = \mathbf{M}_\epsilon^T$ and the natural boundary condition $M_\epsilon^{nn} = 0$ on ∂B_ϵ (see Eq. 11), then Eq. (37) becomes

$$D_T\left(\hat{\mathbf{x}}\right) = -\lim_{\epsilon\to 0}\frac{1}{f'\left(\epsilon\right)}\int_{\partial B_\epsilon}\left\{\frac{6}{E\rho^3}\left[2(1+\nu)\left(M_\epsilon^{nt}\right)^2 + \left(M_\epsilon^{tt}\right)^2\right] - bu_\epsilon\right\}d\partial B_\epsilon\,, \tag{38}$$

In order to obtain the final expression of the Topological Derivative, we need to study the behavior of the integral given by Eq. (38) in relation to ϵ, which may be obtained through an asymptotic analysis of the solution u_ϵ [19, 24].

Therefore, let us consider a boundary-value problem such as the one described by Eq. (11), but now defined in an open ring $A = B_R - \overline{B}_\epsilon \subset \Omega_\epsilon \subset \mathbb{R}^2$ centered at $\hat{\mathbf{x}} \in \Omega$, where $R >> \epsilon$ is such that $R \to 0$, when $\epsilon \to 0$. Then, introducing a coordinate system aligned with the principal stress directions and adopting a polar coordinate system (r,θ) centered at $\hat{\mathbf{x}}$, we have that the following asymptotic expansion for the stress components holds for any $\delta > 0$ (see, for instance, [24])

$$M_\epsilon^{nn} = \frac{S(R)}{2}\left(1-\frac{\epsilon^2}{r^2}\right) + \frac{D(R)}{2}\left(1 - \frac{4\nu}{3+\nu}\frac{\epsilon^2}{r^2} - 3\frac{1-\nu}{3+\nu}\frac{\epsilon^4}{r^4}\right)\cos 2\theta + \mathcal{O}(\epsilon^{1-\delta})\,, \tag{39}$$

$$M_\epsilon^{tt} = \frac{S(R)}{2}\left(1+\frac{\epsilon^2}{r^2}\right) - \frac{D(R)}{2}\left(1 + \frac{4}{3+\nu}\frac{\epsilon^2}{r^2} - 3\frac{1-\nu}{3+\nu}\frac{\epsilon^4}{r^4}\right)\cos 2\theta + \mathcal{O}(\epsilon^{1-\delta})\,, \tag{40}$$

$$M_\epsilon^{nt} = \frac{D(R)}{2}\left(1 - 2\frac{1-\nu}{3+\nu}\frac{\epsilon^2}{r^2} + 3\frac{1-\nu}{3+\nu}\frac{\epsilon^4}{r^4}\right)\sin 2\theta + \mathcal{O}(\epsilon^{1-\delta})\,, \tag{41}$$

where

$$S(R) = m_1(R) + m_2(R) \quad \text{and} \quad D(R) = m_1(R) - m_2(R)\,,$$

being $m_1(R)$ and $m_2(R)$ the principal bending moments, which in the collapsed ring ($\epsilon \to 0$ and $R \to 0$) take the following values

$$\lim_{R\to 0} m_1(R) = m_1 \quad \text{and} \quad \lim_{R\to 0} m_2(R) = m_2\,. \tag{42}$$

Here, m_1 and m_2 are eigenvalues (the principal bending moments) of the generalized stress (bending moment) tensor $\mathbf{M}$ (associated to the original domain without hole Ω) evaluated at the point $\hat{\mathbf{x}} \in \Omega$, that is $\mathbf{M}|_{\hat{\mathbf{x}}}$.

From Eqs. (40, 41) we can respectively compute the components M_ϵ^{tt} and M_ϵ^{nt} on ∂B_ϵ, which may be expressed by

$$M_\epsilon^{tt}\big|_{\partial B_\epsilon} = S(R) - 2\frac{1+\nu}{3+\nu}D(R)\cos 2\theta + \mathcal{O}(\epsilon^{1-\delta})\,, \tag{43}$$

$$M_\epsilon^{nt}\big|_{\partial B_\epsilon} = \frac{2}{3+\nu}D(R)\sin 2\theta + \mathcal{O}(\epsilon^{1-\delta})\,, \tag{44}$$

Next, substituting Eqs. (43, 44) into Eq. (38), we observe that $f'(\epsilon) = -\text{meas}(\partial B_\epsilon) \;\Rightarrow\; f(\epsilon) = -\text{meas}(B_\epsilon)$ and we can finally compute the limit $\epsilon \to 0$ in Eq. (38) which becomes

$$D_T(\hat{\mathbf{x}}) = \frac{6}{E\rho^3}\left[(m_1+m_2)^2 + 2\frac{1+\nu}{3+\nu}(m_1-m_2)^2\right]\,. \tag{45}$$

On the other hand m_1 and m_2 are given by

$$m_{1,2} = \frac{1}{2}\left(\text{tr}\mathbf{M} \pm \sqrt{2\mathbf{M}^D\cdot\mathbf{M}^D}\right)\,, \tag{46}$$

where $\mathbf{M}^D$ is the deviatory stress-tensor, that is

$$\mathbf{M}^D = \mathbf{M} - \frac{1}{2}\text{tr}(\mathbf{M})\,\mathbf{I}\,. \tag{47}$$

Further substituting Eqs. (46, 47) into Eq. (45), we have that

$$D_T(\hat{\mathbf{x}}) = \frac{6}{(3+\nu)E\rho^3}\left[4(1+\nu)\mathbf{M}\cdot\mathbf{M} + (1-\nu)(\text{tr}\mathbf{M})^2\right]\,. \tag{48}$$

Finally, we may rewrite the Topological Derivative as a function of the tensors $\mathbf{M}$ and $\mathbf{E}$ by means of the constitutive equation and a simple manipulation, which leads to

$$D_T(\hat{\mathbf{x}}) = \frac{2}{(3+\nu)}\mathbf{M}\cdot\mathbf{E} + \frac{3\nu+1}{2(3+\nu)(1-\nu)}\text{tr}\mathbf{M}\,\text{tr}\mathbf{E}\,, \tag{49}$$

It should be noted that $\mathbf{M}$ and $\mathbf{E}$ are associated to the original domain Ω (without hole) and that we have assumed $b = 0$.

4 Numerical experiments

We have calculated the Topological Derivative through the Topological-Shape Sensitivity Method (Eq. 3) for Kirchhoff's bending plate problem considering the total potential strain energy as the cost function and the state equation in its weak (variational) form as the constraint. Moreover, from Eq. (48) $D_T(\hat{\mathbf{x}}) \geq 0\,\forall\hat{\mathbf{x}} \in \Omega$. Therefore, the topological derivative can be viewed as an indicator of the degree of non uniformity in the distribution of the generalized stress (bending moments).

This last interpretation of the topological derivative can be used as an alternative method to perform the topology design of plate components: the idea is to introduce holes where $D_T(\hat{\mathbf{x}})$ assumes

the smallest values. Proceeding in this way, we will obtain a new design in which the bending moments should be more uniformly distributed in the new domain. In another words, this approach could be similar to full stressed criterion.

Evidently, to perform an optimal topology design with some physical meaning it will be necessary to take into account more restrictions rather than only the state equations as shown in the present work (for example restrictions in the magnitude of displacements and/or bending moments). However, in this section we only want to show the potentiality of the use of the topological derivative for an appropriate selection of hole localization. Then, the numerical experiments to be described will not incorporate the above constraints.

Based on the algorithm proposed by Cea and co-workers, [4], in [25] was proposed a hard-kill like topology algorithm based on the Topological Derivative, that is, let us consider the following sequence $\{\Omega^j : \text{meas}(\Omega^j) \geq \text{meas}(\hat{\Omega})\}$, where j is the j-th iteration, then:

1. Provide the initial domain Ω and the constraint $\text{meas}(\hat{\Omega})$.
2. While $\text{meas}(\Omega^j) \geq \text{meas}(\hat{\Omega})$ do:
   - **(a)** calculate $D_T\left(\hat{\mathbf{x}}\right)^j$;
   - **(b)** create the holes in the points $\hat{\mathbf{x}}$ corresponding to $\xi_{\text{inf}}^j \leq D_T\left(\hat{\mathbf{x}}\right)^j \leq \xi_{\text{sup}}^j$, where ξ_{inf}^j and ξ_{sup}^j are specified depending on the volume of material to be removed at each iteration;
   - **(c)** define the new domain Ω^{j+1};
   - **(d)** make $j \leftarrow j + 1$.
3. At this stage, we hope to have in hand the desired final topology.

The Topological Derivative depends on the solution of the state equation, u, and its gradient. In this work, u is calculated via the Finite Element Method [18, 38]. More specifically, in the numerical experiments we have adopted the DKT-9 finite element (*Discrete Kirchhoff Triangle*, which is in full detail presented in [2]). Furthermore, $D_T(\hat{\mathbf{x}})$ is evaluated at the nodal points of the finite element mesh, being that we remove the elements that share the node which satisfies $\xi_{\text{inf}} \leq D_T(\hat{\mathbf{x}}_K) \leq \xi_{\text{sup}}$, where $\hat{\mathbf{x}}_K$ is the *K-th* nodal point of the finite element mesh. This procedure, shown in Fig. 1, avoids numerical instability which normally appear in hard-kill like topology algorithm.

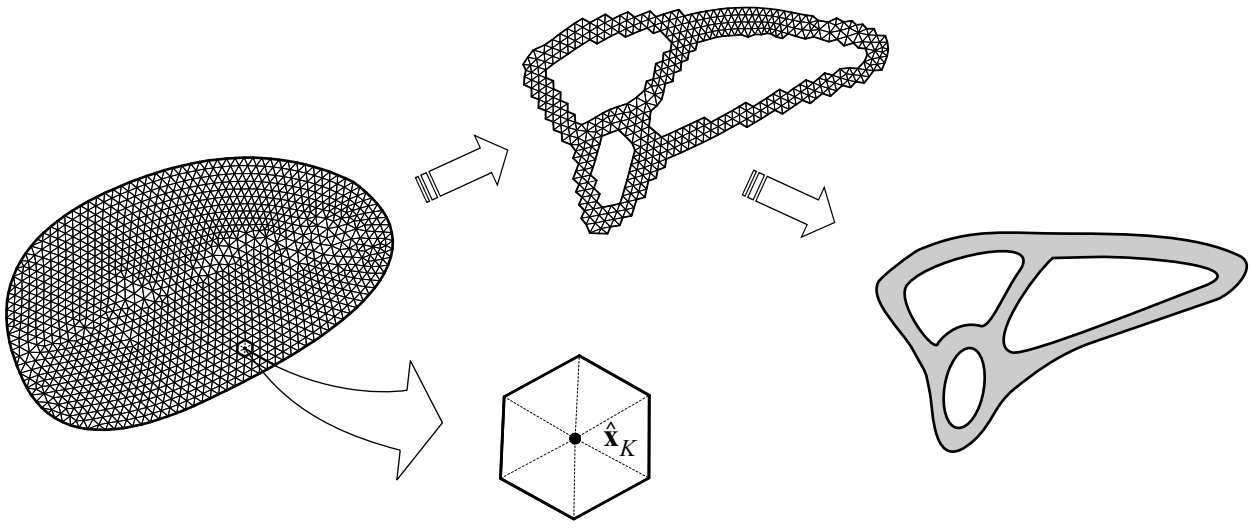

Figure 1: Sketch of the adopted procedure to create the holes in a finite element mesh.

In all the following examples, we remove 1% of material at each step and the Young's modulus $E = 210 \times 10^3\ MPa$, Poisson's ratio $\nu = 1/3$ and thickness $\rho = 5\ mm$ are assumed. Furthermore, the regions that appear in grey are not perturbed and the thick line and the line-dot that appear on the figures are respectively used to denote clamped ($u = \partial u/\partial n = \partial u/\partial t = 0$) and symmetry ($\partial u/\partial n = 0$) boundary conditions.

4.1 Example 1

Let us consider a square plate with two edges free and two edges clamped submitted to a concentrated load $\bar{Q} = 100\,N$ at the corner (Fig. 2(a)). The mesh used to discretize the initial domain $\overline{\Omega} = [0, 1000] \times [0, 1000]\,mm^2$ can be seen in Fig. 2(b).

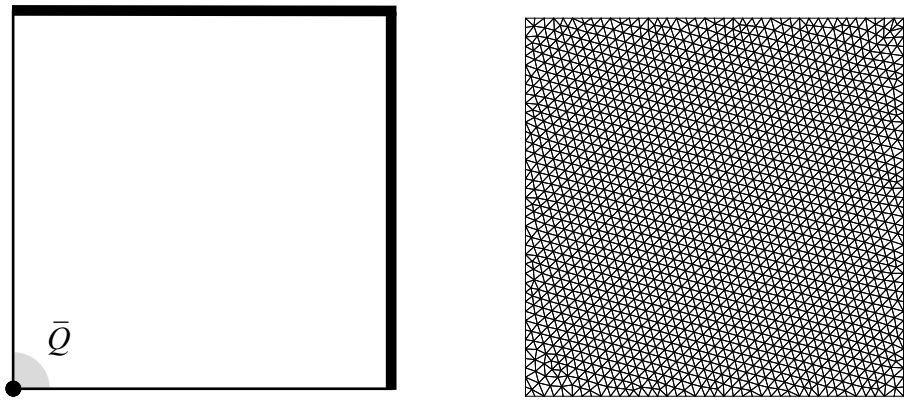

(a) model (b) mesh

Figure 2: Example 1 - model and initial mesh with 3658 finite elements

For the beginning of the process ($j = 0$), the topological derivative and the principal bending moments are presented in Figs. 3(a) and 3(b), respectively. From these figures we observe that the topological derivative enhances the non uniformity in the bending moments distribution.

Considering a stop criterion given by $\text{meas}(\hat{\Omega}) = 0.22\,\text{meas}(\Omega)$, Fig. 4 presents the domain obtained at $j = 75$. In particular, the topological derivative and the principal bending moment (m_1 and m_2) distribution are shown in Figs. 4(a) and 4(b) respectively.

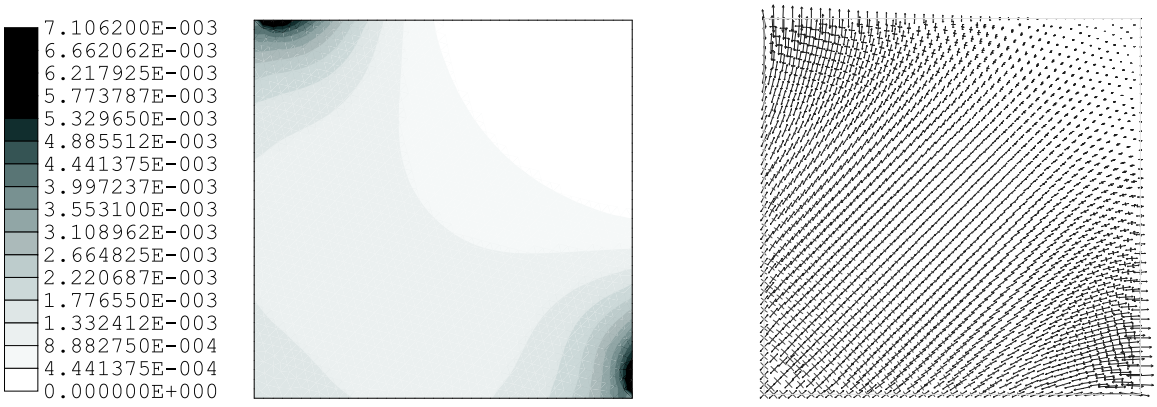

(a) Topological derivative at $j = 0$ (b) m_1 and m_2 at $j = 0$

Figure 3: Example 1 - obtained result at $j = 0$.

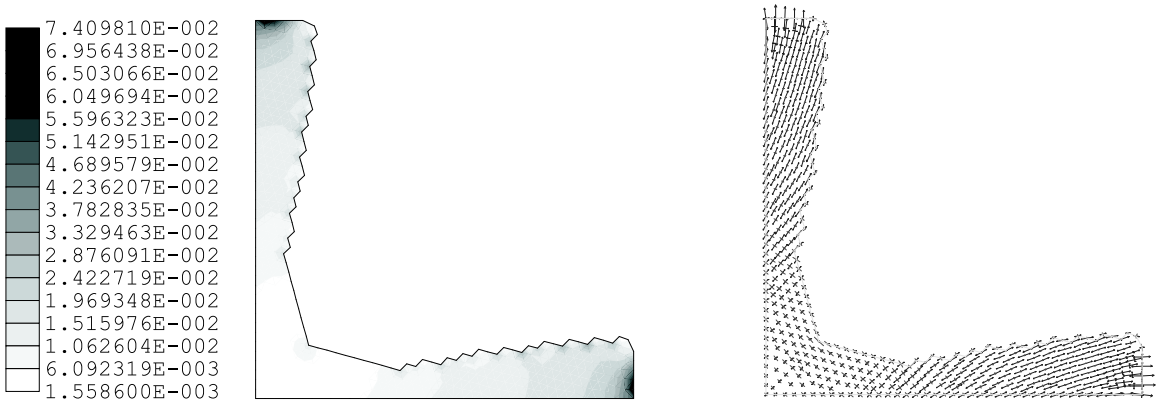

(a) Topological Derivative at $j = 75$

(b) m_1 and m_2 at $j = 75$

Figure 4: Example 1 - obtained result at $j = 75$.

4.2 Example 2

Here, we have a clamped square plate submitted to a concentrated load $\bar{Q} = 100\,N$ at the center (Fig. 5(a)). Due to the symmetry of the problem, the initial domain $\overline{\Omega} = [0, 500] \times [0, 500]\, mm^2$ represents a quarter of the plate, which is discretized as shown in Fig. 5(b). Moreover, taking $\text{meas}(\hat{\Omega}) = 0.60\,\text{meas}\,(\Omega)$ as stop criterion, the final topology obtained at $j = 36$ can be seen in Fig. 6. Here, it is interesting to observe that Liang & Steven found a similar result (see [21] Section 6.3, Fig. 13(c)) using a different approach.

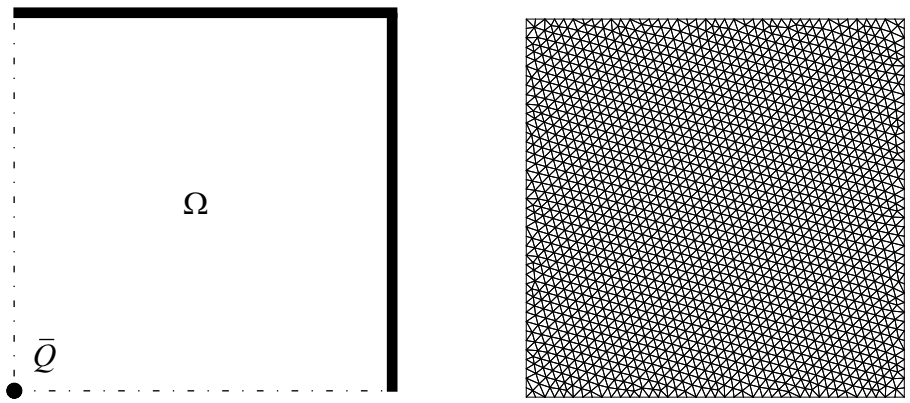

(a) model

(b) mesh

Figure 5: Example 2 - model and initial mesh with 3678 finite elements.

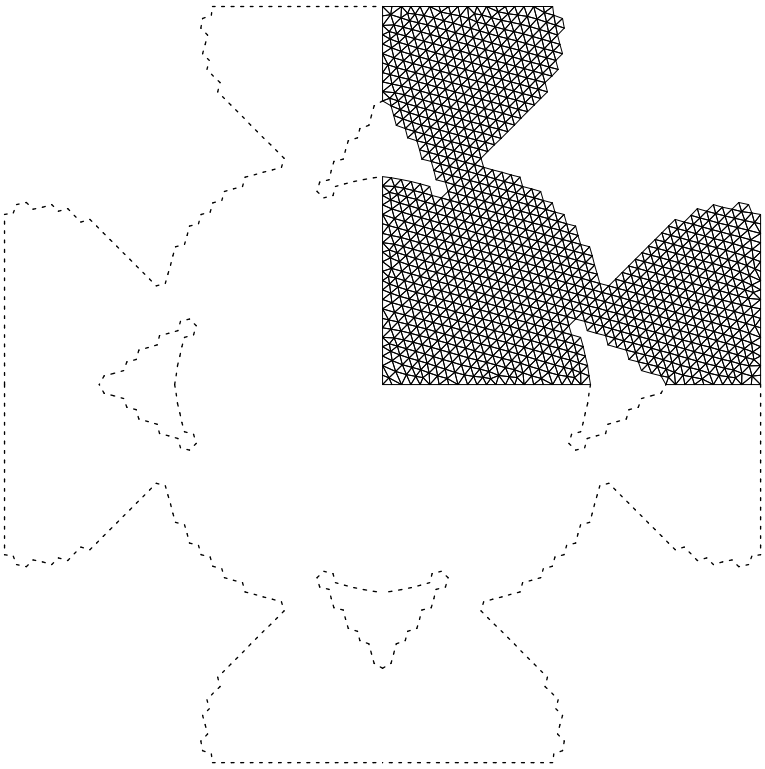

Figure 6: Example 2 - topology at $j = 36$.

4.3 Example 3

Let us consider a flat plates supported by circular columns, submitted to concentrated loads $\bar{Q} = 100\,N$ (see Fig. 7(a) where $R = 50\,mm$ is the column's radius). The initial domain $\overline{\Omega} = [0, 500] \times [0, 500]\,mm^2$ is discretized taking into account the periodic symmetry of the problem, as can be seen in Fig. 7(b).

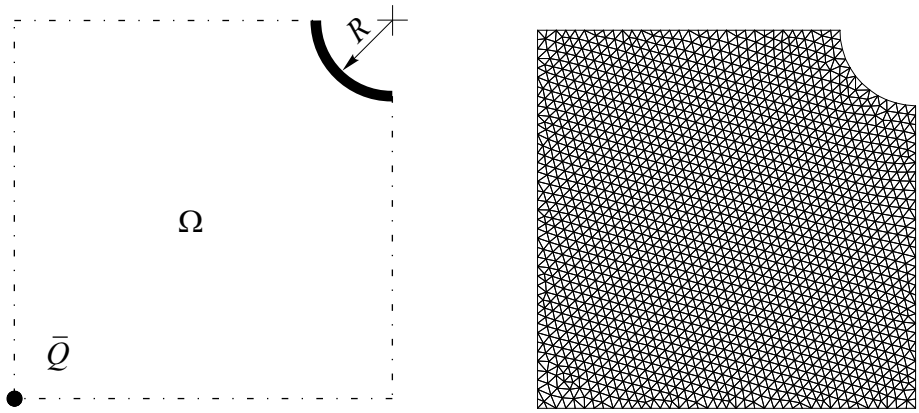

(a) model (b) mesh

Figure 7: Example 3 - model and initial mesh with 3530 finite elements.

For the adopted stop criterion $\text{meas}(\hat{\Omega}) = 0.78\,\text{meas}\,(\Omega)$, the final topology at $j = 19$ is shown in Fig. 8 and the periodicity of the final solution can be seen in Fig. 9.

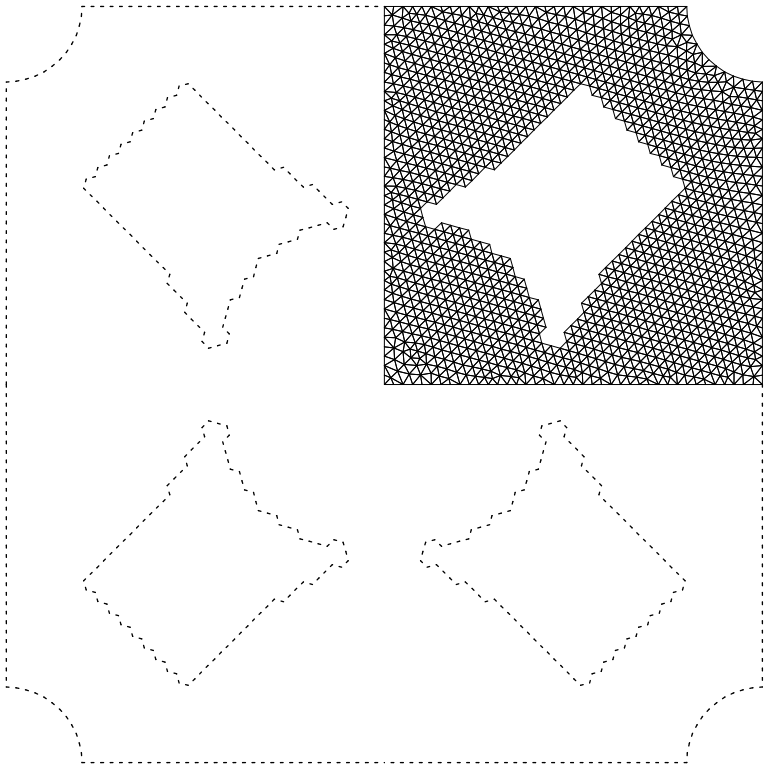

Figure 8: Example 3 - topology at $j = 19$.

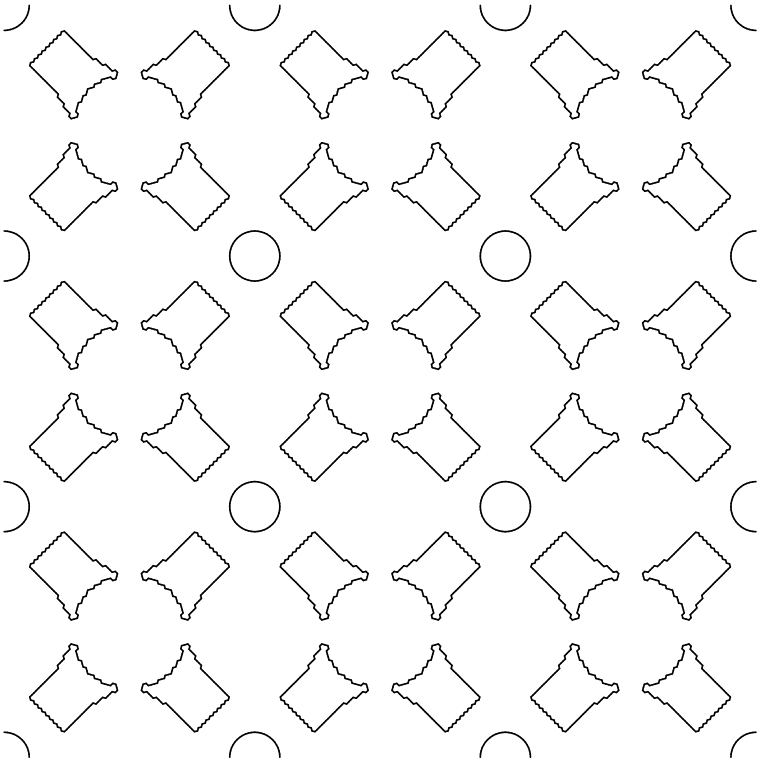

Figure 9: Example 3 - detail of the obtained solution.

4.4 Example 4

In this last example, we have a square plate supported by a column at its center, but now submitted to concentrated loads $\bar{Q} = 100\,N$ at the corners (Fig. 10(a) where $R = 50\,mm$ is the column's radius). Considering the symmetry of the problem, the initial domain $\overline{\Omega} = [0, 500] \times [0, 500]\,mm^2$ is discretized as shown in Fig. (10(b).

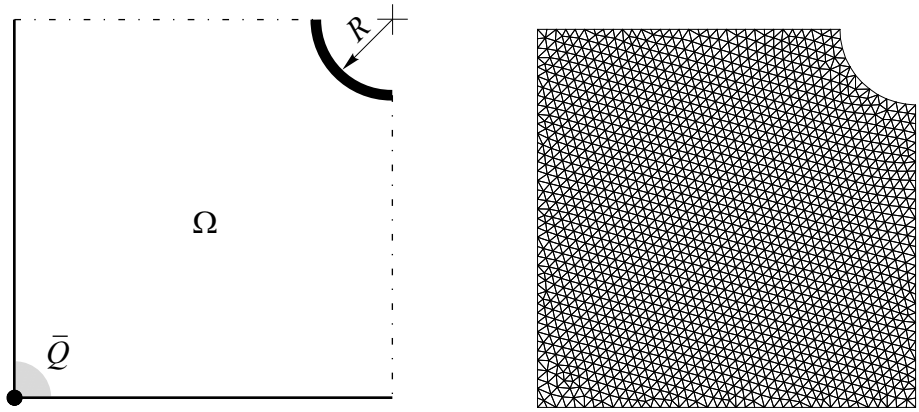

(a) model (b) mesh

Figure 10: Example 4 - model and initial mesh with 3530 finite elements

The Topological Derivative calculated at the beginning of the process ($j = 0$) is shown in Fig. 11(a). As observed, the non uniformity of the bending moment distribution is clearly depicted by this figure in which the isoline of value 1.1×10^{-3} is also presented. Moreover and as expected, at the first step ($j = 1$) the initial hole is localized inside this isoline (see Fig. 11(b)).

Considering $\text{meas}(\hat{\Omega}) = 0.42\,\text{meas}\,(\Omega)$, Fig. (12) presents the domain obtained at the last step ($j = 52$).

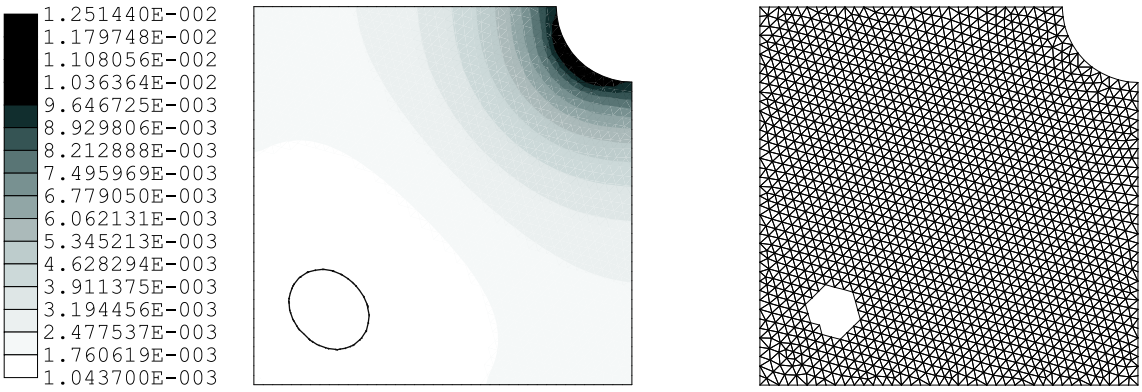

(a) Topological Derivative at $j = 0$ (b) topology at $j = 1$ (first step)

Figure 11: Example 4 - obtained results at $j = 0$ and $j = 1$ (the isoline value is 1.1×10^{-3}).

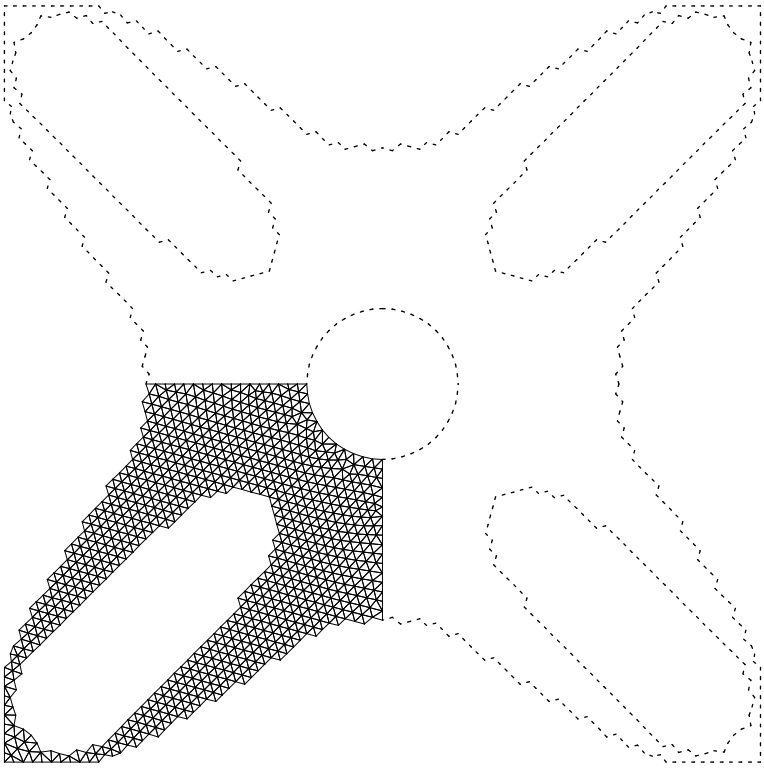

Figure 12: Example 4 - topology at $j = 52$.

5 Conclusions

In this work, the Shape Sensitivity Analysis was employed to evaluate the Topological Derivative of bending elastic plates with different kind of loads, geometry and boundary conditions. The relationship between both concepts was formally established by Theorem 1, leading to the Topological-Shape Sensitivity Method. Therefore, as shown in Section 3.3, results obtained in Shape Sensitivity Analysis (Section 3.2) can be used to perform the Topological Derivative in a constructive way.

In order to illustrate the potentialities of the result given by Theorem 1, the Topological Derivative was calculated for the linear elastic Kirchhoff plate bending problem. Further, we have computed the Topological Derivative for this problem considering the total potential energy as the cost function and the equilibrium equation in its variational form as the constraint, showing that the Topological-Shape Sensitivity Method is, in fact, a framework to obtain the Topological Derivative.

Finally, in Section 4, the Topological Derivative was used to provide an useful information to positioning holes. Nevertheless other strategies using the information provided by the Topological Derivative can be used, we have shown a simple hard-kill like topology algorithm which furnishes satisfactory qualitative results in agreement with those reported in the literature. This fact highlights that the Topological Derivative concept is a tool that can be applied in topology optimization algorithms as pointed out by Eschenauer & Olhoff [5].

Acknowledgments

This research was partly supported by CONICET (Argentina) and the brazilian agencies FINEP/CNPq-PRONEX (664007/1997-0), FAPERJ (E-26/150.712/2003) and CNPq under grant PCI-LNCC/MCT (382616/2002-2). The support from these agencies is greatly appreciated.

References

[1] S. Amstutz, N. Dominguez & B. Samet. Sensitivity Analysis with Respect to the Insertion of Small Inhomogeneities. *Mini-symposium on Topological Sensitivity Analysis: Theory and Applications*, in P. Neittaanmäki [23].

[2] J.-L. Batoz. An Explicit Formulation for an Efficient Triangular Plate-Bending Element. *International Journal for Numerical Methods in Engineering*, **18**:1077-1089, 1982.

[3] J. Céa. Problems of Shape Optimal Design. In Haug & Céa [17].

[4] J. Céa, S. Garreau, Ph. Guillaume & M. Masmoudi. The Shape and Topological Optimizations Connection. *Computer Methods in Applied Mechanics and Engineering*, **188**:713-726, 2000.

[5] H.A. Eschenauer & N. Olhoff. Topology Optimization of Continuum Structures: A Review. *Applied Mechanics Review*, **54**:331-390, 2001.

[6] H.A. Eschenauer, V.V. Kobelev & A. Schumacher. Bubble Method for Topology and Shape Optimization of Structures. *Structural Optimization*, **8**:42-51, 1994.

[7] J.D. Eshelby. The Elastic Energy-Momentum Tensor. *Journal of Elasticity*, **5**:321-335, 1975.

[8] G.R. Feijóo. On The Solution of Inverse Scattering Problems Using the Topological Derivative. *Mini-symposium on Topological Sensitivity Analysis: Theory and Applications*, in P. Neittaanmäki [23].

[9] R.A. Feijóo, A.A. Novotny, E. Taroco & C. Padra. The Topological Derivative for the Poisson's Problem. *Mathematical Models and Methods in Applied Sciences*, **13-12**:1-20, 2003.

[10] R.A. Feijóo, A.A. Novotny, C. Padra & E. Taroco. The Topological-Shape Sensitivity Method and its Application in $2D$ Elasticity. To appear on *Journal of Computational Methods in Sciences and Engineering*.

[11] P. Germain & P. Muller. *Introduction à la Mécanique des Milieux Continus*. Masson, 1994.

[12] S. Garreau, Ph. Guillaume & M. Masmoudi. The Topological Gradient, *Research Report*, UFR MIG, Université Paul Sabatier, Toulouse 3, France, 1998.

[13] S. Garreau, Ph. Guillaume & M. Masmoudi. The Topological Asymptotic for PDE Systems: The Elasticity Case. *SIAM Journal on Control and Optimization*, **39**:1756-1778, 2001.

[14] B.B. Guzina & I. Chikichev. On the Generalized Concept of Topological Sensitivity. *Mini-symposium on Topological Sensitivity Analysis: Theory and Applications*, in P. Neittaanmäki [23].

[15] M. Hassine, S. Jan & M. Masmoudi. From Differential Calculus to 0-1 Optimization. *Mini-symposium on Topological Sensitivity Analysis: Theory and Applications*, in P. Neittaanmäki [23].

[16] E.J. Haug, K.K. Choi & V. Komkov. *Design Sensitivity Analysis of Structural Systems*. Academic Press, 1986.

[17] E.J. Haug & J. Céa. Proceedings: *Optimization of Distributed Parameters Structures*, Iowa, EUA, 1981.

[18] T.J.R. Hughes. *The Finite Element Method - Linear Static and Dynamic Finite Element Analysis*. Prentice-Hall, 1987.

[19] A.M. Il'in. *Matching of Asymptotic Expansions of Solutions of Boundary Value Problems*. Translations of Mathematical Monographs vol. 102. AMS, Providence, 1992.

[20] T. Lewiński & J. Sokolowski. Energy change due to the appearance of cavities in elastic solids. *International Journal of Solids and Structures*, **40**:1765-1803, 2003.

[21] Q.Q. Liang & G.P. Steven. A Performance-Based Optimization Method for Topology Design of Continuum Structures with Mean Compliance Constraints. *Computer Methods in Applied Mechanics and Engineering*, **191**:1471-1489, 2002.

[22] F. Murat & J. Simon. *Sur le Contrôle par un Domaine Géométrique*. Thesis, Université Pierre et Marie Curie, Paris VI, França, 1976.

[23] P. Neittaanmäki, T. Rossi, S. Korotov, E. Oñate, J. Périaux & D. Knörzer (eds.), Proceedings: *ECCOMAS 2004 - European Congress on Computational Methods in Applied Sciences and Engineering*, Jyväskylä, 24-28 July, 2004.

[24] A.A. Novotny. *Análise de Sensibilidade Topológica*. Ph. D. Thesis, LNCC/MCT, Petrópolis - RJ, Brasil, 2003 (http://www.lncc.br/∼novotny/principal.htm).

[25] A.A. Novotny, R.A. Feijóo, C. Padra & E. Taroco. Topological Sensitivity Analysis. *Computer Methods in Applied Mechanics and Engineering*, **192**:803-829, 2003.

[26] A.A. Novotny, T.G. Felipe, R.A. Feijo, C. Padra & E. Taroco. Topological-Shape Sensitivity Method Applied to Inverse Poisson's Conductivity Problem. Inverse Problems, Design and Optimization - IPDO Synposium, Rio de Janeiro, Brasil, 2004.

[27] A.A. Novotnyy, C. Padra, R.A. Feijóo & E. Taroco. The Topological-Shape Sensitivity Method. *Mini-symposium on Topological Sensitivity Analysis: Theory and Applications*, in P. Neittaanmäki [23].

[28] C. Padra, A.A. Novotnyy, R.A. Feijóo & E.Taroco. The Topological-Shape Sensitivity Method and its Applications in Topology Design and Inverse Problems. *Mini-symposium on Topological Sensitivity Analysis: Theory and Applications*, in P. Neittaanmäki [23].

[29] O. Pironneau. *Optimal Shape Design for Elliptic Systems*. Springer-Verlag, 1984.

[30] O. Pironneau. Derivatives with Respect to Piecewise Constant Coefficients of a PDE with Application to Calibration. *Mini-symposium on Topological Sensitivity Analysis: Theory and Applications*, in P. Neittaanmäki [23].

[31] A. Schumacher. Topologieoptimierung von Bauteilstrukturen unter Verwendung von Lochpositionierungkriterien, Ph.D. Thesis, Universität-Gesamthochschule-Siegen, Siegen, 1995.

[32] J. Sokolowski. Asymptotic Analysis and Shape Optimization in Elasticity. *Mini-symposium on Topological Sensitivity Analysis: Theory and Applications*, in P. Neittaanmäki [23].

[33] J. Sokolowski & A. Żochowski. On the Topological Derivative in Shape Optimization. Research Report n. 3170, INRIA-Lorraine, France, 1997. *SIAM Journal on Control and Optimization*, **37**:1251-1272, 1999.

[34] J. Sokolowski & A. Żochowski. Topological Derivatives for Elliptic Problems. *Inverse Problems*, **15**:123-134, 1999.

[35] J. Sokolowski & A. Żochowski. Topological Derivatives for Contact Problems. *Mini-symposium on Topological Sensitivity Analysis: Theory and Applications*, in P. Neittaanmäki [23].

[36] J. Sokolowski & J.-P. Zolésio. *Introduction to Shape Optimization - Shape Sensitivity Analysis*. Springer-Verlag, 1992.

[37] E. Taroco. G.C. Buscaglia & R.A. Feijóo. Second-Order Shape Sensitivity Analysis for Nonlinear Problems. *Structural Optimization*, **15**:101-113, 1998.

[38] O.C. Zienkiewicz & R.L. Taylor. *The Finite Element Method*. McGraw Hill, 1989.

[39] J.-P. Zolézio. The Material Derivative (or Speed) Method for Shape Optimization. In Haug & Céa [17].